Prediction of bird-beak configuration in thoracic endovascular aortic repair preoperatively using patient-specific finite element simulations

Negin Shahbazian, PhD,[a] David A. Romero, PhD,[a] Thomas L. Forbes, MD,[b] *and* Cristina H. Amon, ScD,[a,c] *Toronto, ON, Canada*

ABSTRACT

Objectives: Formation of bird-beak configuration in thoracic endovascular aortic repair (TEVAR) has been shown to be correlated with the risk of complications such as type Ia endoleaks, stent graft migration, and collapse. The aim of this study was to use patient-specific computational simulations of TEVAR to predict the formation of bird-beak configuration preoperatively.

Methods: Patient-specific TEVAR computational simulations are developed using a retrospective cohort of patients treated for thoracic aortic aneurysm. The preoperative computed tomography images were segmented to develop three-dimensional geometry of the thoracic aorta. These geometries were used in finite element simulations of stent graft deployment during TEVAR. Simulated results were compared against the postoperative computed tomography images to assess the accuracy of simulations in predicting the proximal position of a deployed stent graft and presence of bird-beak. In cases with a bird-beak configuration, the length and angle of the bird-beak were measured and compared between the simulated and postoperative results.

Results: Twelve TEVAR patient cases were simulated. Computational simulations were able to accurately predict whether the proximal stent graft was fully apposed, proximal bare stents were protruded, or bird-beak configuration was present. In three cases with bird-beak configuration, simulations predicted the length and angle of the bird-beak with less than 10% and 24% error, respectively. Other factors such as a small aortic arch angle, small oversizing value, and landing zones close to the arch apex may have played a role in formation of bird-beak in these patients.

Conclusions: Computational simulations of TEVAR accurately predicted the proximal position of a deployed stent graft and the presence of bird-beak preoperatively. The computational models were able to predict the length and angle of bird-beak configurations with good accuracy. These simulations can provide insight into the surgical planning process with the goal of minimizing bird-beak occurrence. (JVS—Vascular Science 2023;4:100108.)

Clinical Relevance: Finite element analysis is a noninvasive method for simulation and prediction of thoracic endovascular aortic repair (TEVAR) outcomes. In this study, a computational approach for patient-specific simulations of TEVAR was implemented to accurately predict bird-beak configuration preoperatively. In addition, the length and angle of bird-beak configurations, which have been shown in previous studies to be correlated with bird-beak adverse events, were predicted with good accuracy. This computational approach is clinically significant as it has the potential to enhance TEVAR surgical planning capabilities with the goal of minimizing bird-beak occurrence. For patients with risk of bird-beaking, additional emphasis can be placed on optimal stent graft oversizing and device selection.

Keywords: TEVAR; Bird-beak configuration; Thoracic aortic aneurysm; Computational simulations; Finite elements

Poor apposition of the proximal stent graft to the aortic wall during thoracic endovascular aortic repair (TEVAR) can produce a wedge-shaped gap known as bird-beak configuration (Fig 1), which can lead to various secondary complications. Some of these complications include endoleak, stent graft migration, device collapse, or

From the Department of Mechanical and Industrial Engineering,[a] Division of Vascular Surgery, Department of Surgery, Peter Munk Cardiac Centre, University Health Network,[b] and Department of Mechanical and Industrial Engineering, Institute of Biomedical Engineering,[c] University of Toronto.

This project has received funding from the Natural Sciences and Engineering Research Council of Canada and the Peter Munk Cardiac Centre Innovation Grant. The Natural Sciences and Engineering Research Council of Canada and the Peter Munk Cardiac Centre had no involvement in the study design, analysis, and interpretation of data. Patient data have been collected from a retrospective cohort of patients treated at the Peter Munk Cardiac Centre.

Author conflict of interest: none.

Correspondence: Negin Shahbazian, PhD, Department of Mechanical and Industrial Engineering, University of Toronto, 5 King's College Rd, Toronto, ON M5S 3G8, Canada (e-mail: negin.shahbazian@mail.utoronto.ca).

The editors and reviewers of this article have no relevant financial relationships to disclose per the Journal policy that requires reviewers to decline review of any manuscript for which they may have a conflict of interest.

2666-3503

https://doi.org/10.1016/j.jvssci.2023.100108

infolding.[1-4] Bird-beak length and angle, defined in Fig 1, have been used to determine its clinical significance and are correlated with the risk of bird-beak-related complications.[2,4-6] Several factors including landing zone, distal arch angle, and stent graft stiffness, and the used delivery system have been identified to play a role in bird-beak formation.[3,7,8] In a parametric computational study, finite element simulations of TEVAR were used to show that aortic geometry, stent graft design parameters, and landing zone can influence bird-beak.[9]

Prediction of surgical complications preoperatively can be helpful in modifying surgical plans accordingly and minimizing the occurrence of complication. Computational simulations of TEVAR have the potential to predict surgical outcomes preoperatively and have been used in several studies[10-17] to achieve satisfactory numerical results for the application under investigation. The aim of this study is to employ a previously developed computational framework for simulations of TEVAR[18] to predict the proximal position of the deployed stent graft and bird-beak configuration formation preoperatively. The accuracy of this framework in predicting the bird-beak presence and geometric size is assessed using patient-specific geometries reconstructed from postoperative imaging of a retrospective cohort of TEVAR patients.

ARTICLE HIGHLIGHTS

- **Type of Research:** Basic science
- **Key Findings:** The proposed patient-specific computational simulations of TEVAR can accurately predict the final deployment position of the stent graft and bird-beak configuration preoperatively.
- **Take Home Message:** Finite element analysis is a noninvasive method for simulating TEVAR scenarios and prediction of surgical outcomes. The proposed framework can predict the presence or absence of bird-beak in TEVAR preoperatively. Additionally, the simulations can predict the length and angle of the bird-beak deformity with over 90% and 76% accuracy, respectively. This computational approach can provide insight into the preoperative planning process and has the potential to enhance surgical planning capabilities with the goal of minimizing bird-beak occurrence.

MATERIALS AND METHODS

Computed tomography (CT) or magnetic resonance (MR) images of thoracic aortic aneurysm patients treated with TEVAR, with and without bird-beak configurations, were collected. The preoperative geometric configuration of the thoracic aorta was segmented to obtain a three-dimensional geometry, which was then used to develop computational simulations of stent graft deployment in the aorta. The position of the deployed stent graft was assessed in the simulated results and compared against the postoperative images. In cases with a bird-beak configuration, the geometric characteristics of the bird-beak gap were measured and compared between the postoperative and simulated results.

Patient inclusion criteria. After institutional research ethics approval, a retrospective study of TEVAR patients was conducted. All elective TEVAR cases (except those that met the exclusion criteria) for thoracic aortic aneurysm repair at Toronto General Hospital from October 1, 2009, to September 30, 2017, and any corresponding follow-up for these patients to September 30, 2019, were reviewed. TEVAR patients with Marfan syndrome, patients treated for aortic dissection and blunt aortic injury, patients with myotic thoracic aortic aneurysm, and patients who lacked preoperative or postoperative CT or MR imaging or scans with sufficient resolution for segmentation were excluded from the study.

A total of 145 patients were selected for preliminary screening (Table I). All patients with a genetic history (including connective tissue disorders Marfan syndrome, Ehlers-Danlos syndrome, and Loey-Dietz syndrome) and patients with proximal landing zones[19] 5 to 9 were eliminated. Some patients did not have usable CT images with sufficient resolution. At least eight patients did not have pre- or postoperative CT scans. In addition, six patients had previous aortic prosthetics at the time of the TEVAR that were eliminated from the study because accurate computational modeling of a pre-existing device was not in scope for our previously developed simulation framework.[18] Computational simulation of the pre-existing stent grafts would have required the preoperative CT images of the initial surgery, as well as a method to account for aortic remodeling in the time leading up to the subsequent TEVAR. Cook Medical (Cook Medical) devices were predominantly used in our center. In addition, our previously developed simulation framework includes methods to develop computational models of Cook Medical devices as well as their delivery and deployment. Hence, 10 patients with devices from other manufacturers were considered out of scope for this study. In addition, eight patients with unreferenced or custom Cook Medical device types were considered out of scope. Consequently, 34 of 145 patients without a genetic history or previous aortic prosthetics, with TEVAR landing zones 0 to 4, and referenced Cook Medical stent grafts were identified for more in-depth screening.[20] The details of patient inclusion criteria are listed in Table I.

No patients with landing zone 0 or 1 met the inclusion criteria. The number of in-scope patients per TEVAR landing zones 2, 3, and 4 was 9, 11, and 14, respectively. Of the 34 patients who met the inclusion criteria, 20

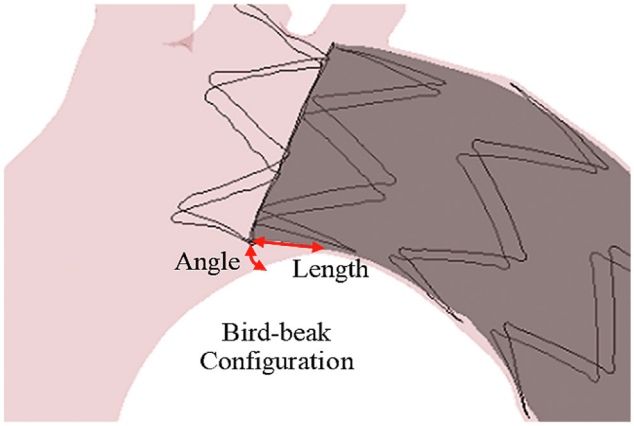

Fig 1. Definition of bird-beak configuration, bird-beak length, and angle.

Table I. Summary of patient inclusion criteria

N	Inclusion/exclusion criteria
145	Total
111	Excluded
82	With genetic history and/or within proximal landing zones 5 to 9
18	Out-of-scope device types
4	Previous aortic prosthetics
7	Unavailable pre- or postoperative CT or MR images
34	Included (landing zones 0 to 4, known Cook devices, no genetic history)
20	With Cook Zenith Alpha stent grafts
14	With Cook Zenith TX2 stent grafts

CT, Computed tomography; *MR*, magnetic resonance.

had Cook Zenith Alpha and 14 had Cook Zenith TX2 (Cook Medical) thoracic stent grafts. Surgery angiography images, pre- and postoperative MR or CT images, and surgical notes were reviewed to identify patients with bird-beak configurations. Twelve patient cases (5 in zone 2, 4 in zone 3, and 3 in zone 3) were identified and selected for engineering analysis and computational simulations. The rationale behind selecting these 12 patients was to include several patients within each TEVAR landing zone with different conditions of proximal stent graft to aorta apposition. All the patients with bird-beak configuration (N = 3) and unopposed proximal bare stents (N = 4), which were only observed in zones 2 and 3, were included. In addition, in each of zones 2 and 3, one patient with complete proximal stent graft apposition was included. All patients with a TEVAR landing zone 4 had complete proximal stent graft apposition, of whom two patients with Zenith Alpha and one patient with Zenith TX2 devices were selected for simulation. Selection of the patients provided sufficient variability in parameters such as oversizing and aortic geometry for the purpose of analysis. In addition, simulating 12 patient cases was feasible for study timelines. Anonymized pre- and postoperative CT or MR images of selected patients were collected for segmentation.

Aortic geometry and segmentation. The preoperative CT images of selected patients were segmented using the open-source software 3D Slicer (Slicer) using the Vascular Modelling Tool Kit (VMTK) library.[21] First, the aorta was segmented by local thresholding followed by the discrete flying edges algorithm[22] to transform the segmented geometry into a surface model. Then any surrounding structures that may have been included in the segmentation were manually cut and deleted using the island elimination method. Any additional adjustments of the segmented aorta were implemented manually using the paint and erase tools in the axial and sagittal views. This step is directly related to the local intensity threshold set in the first step of the segmentation. If the selected threshold is relatively small, it can help with isolating the aorta from the surrounding structure, but in turn result in shrinking the aorta, which warrants manual adjustments. If the selected threshold is large, it can result in segmenting a more accurate aorta volume but include unwanted surrounding structures as well. This manual step is mainly used in the descending thoracic aorta where the surrounding structures such as the spine and branching vessels need to be eliminated from the segmented aorta geometry. Because all bird-beak cases in our patient cohort occurred more proximally and closer to the apex of the arch, manual adjustments did not occur near the bird-beak site. The segmentation is then followed by surface smoothing using the joint smoothing algorithm that tends to maintain the segmented volume compared with smoothing algorithms such as Gaussian that shrink the volume.[23] Finally, using the VMTK module, the vessel centerline curve was extracted. The desired number of nodes along the centerline was determined, and the coordinates of these nodes were exported for use in the simulation. To create a hollow shell with open ends, the ends of the vessel adjacent to the aortic root and the diaphragm, and the supra-aortic branch vessels were clipped using Meshmixer (Autodesk). An example of the segmented aorta is shown in Fig 2.

The hollow vessel geometry with clipped ends was imported into HyperMesh (Altair) for mesh generation. Mesh convergence and independence test was carried out with focus on displacements and stresses near the proximal landing zone of the stent graft during TEVAR. Triangular shell elements with 1.5 mm size were used, which resulted in an average of approximately 20,000

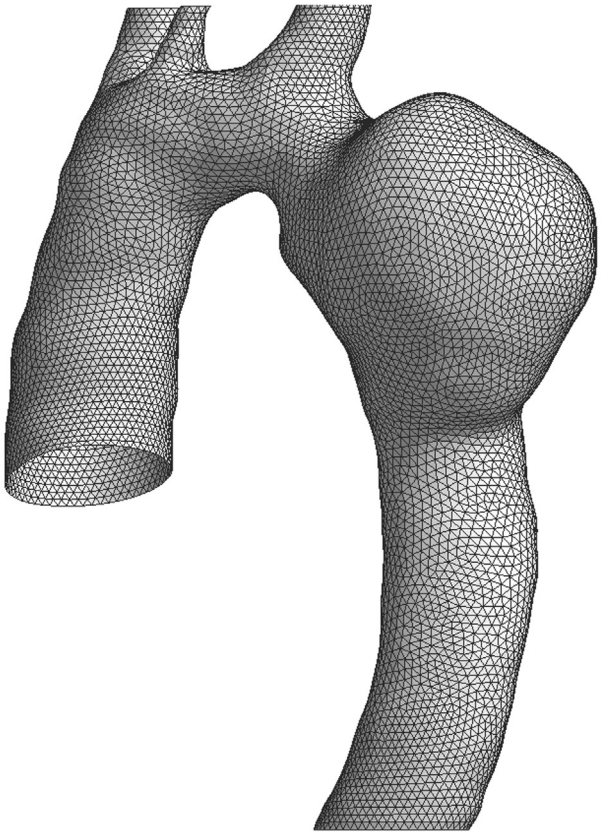

Fig 2. Sample aorta segmentation with representative mesh.

elements in the aortic geometry. A representative mesh is shown in Fig 2.

Computational modeling. Computational models of the stent graft configurations deployed for each patient case were generated in-house using SolidWorks (Dassault Systèmes Solid Works Corp) in accordance with Cook device specifications.[24] The stent grafts were meshed in HyperMesh using 1 mm quadratic shell elements for the graft and 0.6 mm circular beam elements for the stents. On average, the grafts and stents consisted of approximately 8000 and 2600 elements, respectively. Note that the exact number of elements varied based on vessel size and stent graft configuration. A straight Lunderquist guidewire (Cook Medical) was used in all simulation cases that was meshed using 1 mm circular beam elements. Based on the type of device used in each patient, the material properties of the graft and stents were modified accordingly in each simulation.

A previously defined age-dependent constitutive Mooney-Rivlin material model[18] for thoracic aortic tissue was used for the aorta. The selected material model is defined for nonaneurysmal tissue. Because the focus of this study is prediction of the proximal position of the deployed stent graft and bird-beak configuration formation that occurs along the proximal landing zone with nonaneurysmal tissue, the use of such a material model was deemed appropriate. In addition, in another study,[9] it was shown that age-related changes in aortic tissue properties had an insignificant impact on the formation of bird-beak configuration, and using aortic tissue properties defined for different age ranges does not impact simulation results when considering bird-beak. Hence, only the tissue properties of one age group (71-78 years) from reference[18] were used in all the simulations, regardless of patient age.

Simulation steps. The finite element software LS-Dyna (LSTC) with an explicit time integration algorithm was used for the computational simulations. Before TEVAR simulations, the aortic geometry was prestressed to a zero-pressure configuration, following an iterative process defined by Raghavan et al.[25] During this process, the initial segmented aortic geometry was first assumed to be stress free. This initial vessel configuration was then pressurized at a mean physiological blood pressure of 93 mm Hg.[26] The nodal displacements between the initial and inflated states were calculated and subtracted from the initial state to obtain a deflated geometry. Repeating the process starting with the deflated state instead of the initial configuration, the nodal displacements were incrementally subtracted from the initial state until the residual difference was at its minimum, at which point the prestressed geometry at zero pressure was obtained.

Stent graft deployment in TEVAR cases was simulated following a previously established computational framework.[18] Briefly, the stent graft was first crimped and tied to the guidewire. The guidewire was rigidly deformed and placed on the location of the vessel centerline, using the extracted centerline coordinates previously obtained from VMTK. The constraints on the guidewire nodes were then terminated, allowing the guidewire to deform and expand toward the larger curvature of the aorta, while carrying the crimped stent graft. After the position of the guidewire within the aorta was stabilized, the stent graft was expanded and deployed. The computational models did not include navigation of the delivery system inside the aorta. Therefore, the movement of stent graft upon deployment was not considered in the simulations as the stent graft was directly deployed in the desired final location within the aorta. Furthermore, because the navigation process was bypassed, and the guidewire was rigidly deformed by the simulation algorithm and its nodes were superimposed on the vessel centerline location, a curved guidewire would have behaved identically to the used straight guidewire. The aorta was pressurized at a mean physiological blood pressure of 93 mm Hg[26] during the simulations. The nodes at the proximal and distal ends of the aorta geometry were constrained translationally. Numerical damping was applied for

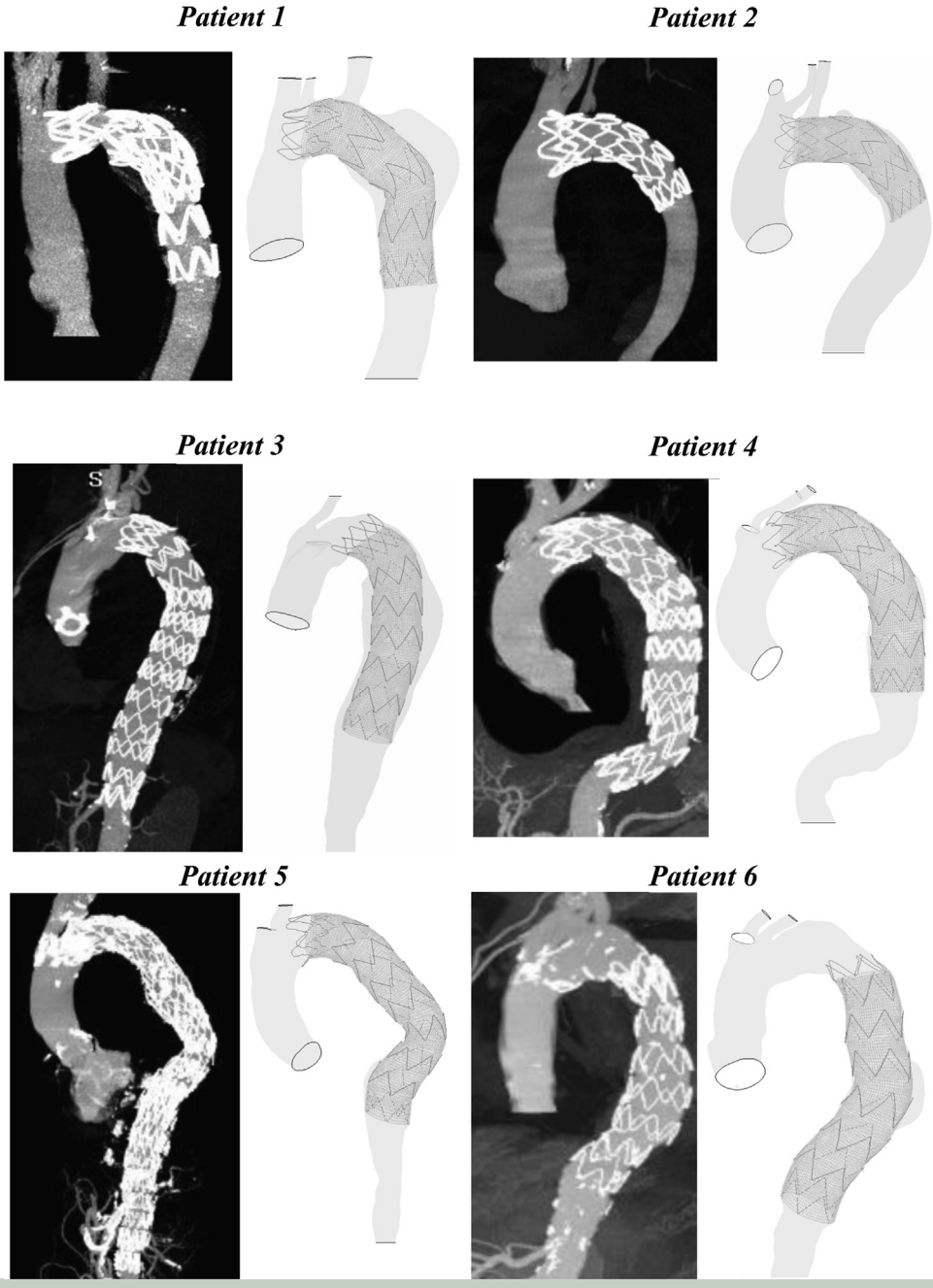

Fig 3. Postoperative 3D reconstruction (left) and simulated results (right) of patients 1 to 6.

each part to decrease instability and simulate the damping effect of surrounding tissues. A sensitivity analysis was completed to determine the optimal damping factors by testing numerical damping values between 10% and 20% of critical, which is a commonly used range.[27] Friction was considered between parts based on friction measurements presented in two studies using benchtop testing.[28,29] Coefficients of friction applied between the guidewire and vessel, stents and vessel, and graft and vessel were 0.05, 0.05, and 0.145, respectively. The geometry segmentation and simulation setup time for each patient is approximately 20 hours. The computational time for each simulation is up to 2 hours using a high-performance computing server with 12 cores. Carrying out the simulations requires expertise in the finite element method and geometry segmentation.

RESULTS

Simulation validation. Twelve TEVAR patient cases were simulated to deploy the stent graft in each case. In cases with multiple stent grafts, the most proximal piece was used in the simulation. To validate the

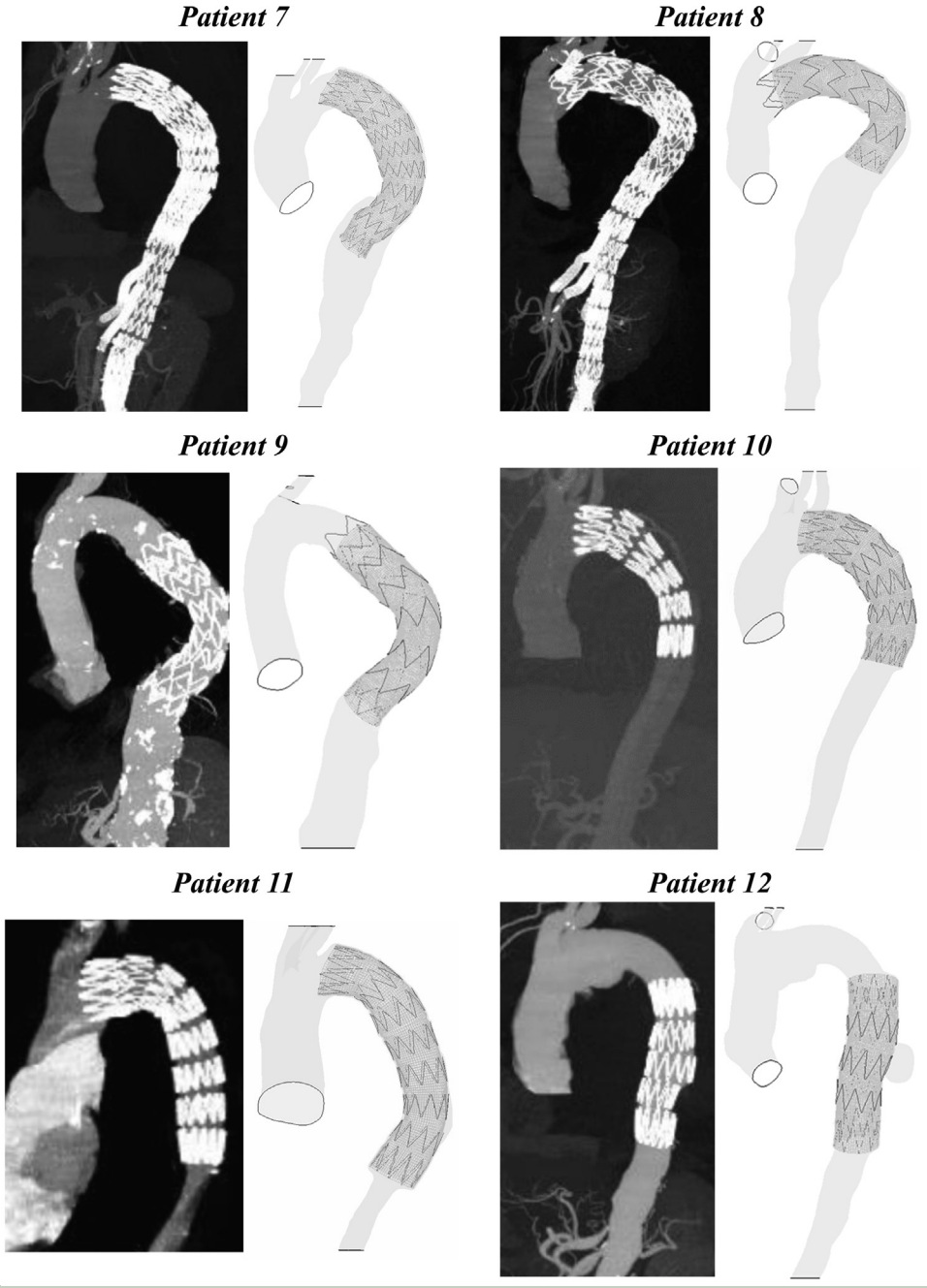

Fig 4. Postoperative 3D reconstruction (left) and simulated results (right) of patients 7 to 12.

simulation results, they were compared against the first postoperative CT images. Using the Aquarius iNtuition software (TeraRecon), a 3D reconstruction of the postoperative CT images was generated by volume rendering of the images into 3D structures. For each patient, the 3D reconstruction of postoperative CT images was assessed, and the proximal position of the deployed stent graft was captured at the sagittal plane or the approximated arch cross-sectional plane (depending on the arch orientation).

Classification of patient cases using proximal stent graft apposition. In the literature, bird-beak configuration is generally defined as the gap between the unapposed endograft and the vessel, and its length is measured from the tip of the graft. However, a few studies measured the length of the bird-beak configuration from the tip of the proximal stents to the end of the unapposed section.[30-32] For instance, Boufi et al[30] identified bird-beak configuration as protrusion of stent with a length greater than 5 mm. In this study, it is

Table II. Patient and stent graft characteristics

Patient	Proximal landing zone	Stent graft type	Age at procedure	α,°	Oversizing, %	Proximal stent graft apposition
1	2	Zenith Alpha	45	61.42	24	Unapposed proximal bare stents
2	2	Zenith Alpha	57	78.66	12	Unapposed proximal bare stents
3	3	Zenith Alpha	68	58.6	8	Unapposed proximal bare stents
4	3	Zenith Alpha	72	58.92	18	Unapposed proximal bare stents
5	4	Zenith Alpha	77	65.09	17	Fully apposed
6	3	Zenith Alpha	78	58.97	30	Fully apposed
7	3	Zenith TX2	67	61.68	5	Bird-beak configuration
8	2	Zenith Alpha	83	67.67	18	Fully apposed
9	4	Zenith Alpha	84	70.24	18	Fully apposed
10	2	Zenith TX2	38	73.59	11	Bird-beak configuration
11	2	Zenith TX2	57	55.82	21	Bird-beak configuration
12	4	Zenith TX2	80	64.97	28	Fully apposed

specified whether the stent graft was fully apposed, protrusion of proximal bare stents was observed, or bird-beak configuration (unapposed endograft) was present. Using these three classification categories would allow us to assess how accurately the simulations can predict the proximal position of the stent graft after deployment. The simulation results were compared with the 3D reconstruction of postoperative CT images presented in Figs 3 and 4. The simulated and postoperative results were visually assessed to determine the proximal position of the deployed stent graft using one of three classification categories. Bird-beak configuration was observed in 3 of 12 patients. The condition of the proximal stent graft apposition for each patient case is presented in Table II.

Bird-beak contributing factors. The age range for the 12 simulated patients is from 38 to 84 years. For each patient, the aortic arch angle α[31] was measured as the angle between the lines that connects the arch apex to the centerline of the ascending and descending aorta at the level of the bifurcation of the pulmonary trunk. Oversizing was calculated for each patient as the percentage difference between the stent graft and vessel outer diameters. In our previous study,[9] correlations were found between bird-beak configuration and landing zone, stent graft oversizing, and aortic arch angle. Therefore, these factors were assessed for each patient case. A summary of patient data and stent graft characteristics for each case is presented in Table II.

Bird-beak configuration geometry measurement. For the three patient cases with bird-beak configurations, the length and angle of the bird-beak were measured in the simulated results and postoperative CT images. In the simulated results, bird-beak length and angle were obtained using the measurement tools in LS-Dyna, by their two-dimensional projection on a plane that passed through the midline of the protruded portion of the graft, normal to the graft surface. In the postoperative results, the 3D reconstruction of the CT images (at the sagittal plane or the approximated arch cross-sectional plane) was first scaled using the height of the stent as a reference. The geometry measurements were taken after scaling. In the CT images, bird-beak length and angle were measured twice by the same observer with measurement being carried out approximately 1 week apart. Intraobserver reliability tests were performed using Lin's concordance correlation coefficient method.[33] Lin's concordance correlation coefficient was calculated for bird-beak length and angle as 0.97 and 0.91, respectively, where values below 0.9 are considered poor agreement, 0.9 to 0.95 are moderate, 0.95 to 0.99 are significant agreement, and values above 0.99 indicate nearly perfect agreement. Intra- and interobserver reliability tests were not applicable in the simulated results because the measurements were performed computationally. The percentage of error for the simulated results compared with postoperative images was calculated for each bird-beak length and angle measurement. These results are presented in Table III.

DISCUSSION

Bird-beak configurations were observed in patients 7, 10, and 11. It is speculative that the formation of bird-beak in these patients is related to stent graft selection as Zenith TX2 devices were used in all three. From the 14 investigated patient cases with Cook Zenith TX2 devices, 4 were with bird-beak configuration (29%). One of these cases was not simulated due to unavailability of preoperative CT images. This is while bird-beak was not detected in any of the cases with Cook Zenith Alpha devices. Some of the design differences between Zenith TX2 and Zenith Alpha include the lack of proximal bare stents and a greater number of peaks and valleys in

Table III. Simulated vs postoperative measurement of bird-beak length and angle in three patients with bird-beak configuration

	Bird-beak length, mm			Bird-beak angle, °		
Patient	Simulated	Postoperative CT	Difference, %	Simulated	Postoperative CT	Difference, %
7	12.8	12.1	5.7	38.8	31.4	23.5
10	7.4	8.1	−9.4	24.1	29.1	−20.7
11	9.3	10.2	−9.7	50.6	58	−14.6

CT, Computed tomography.

each stent segment in the Zenith TX2 device.[24] The Zenith TX2 stents are made of 316L stainless steel that is a stiffer material than Nitinol used in Zenith Alpha. The stiffness of 316L stainless steel used in the Zenith TX2 device can contribute to its poor overall bending and conformability.

Proximal bare stent components have been shown in previous studies[34,35] to reduce the occurrence of bird-beak configuration, as they improve stent graft's conformability to the aorta. In a study by Kudo et al[34] investigating 105 TEVAR patients with different stent graft types, it was shown that in the first postoperative follow-up, all bird-beak cases were found in patients with stent grafts without proximal bare stents. No bird-beak cases were found in patients with proximal bare stents. In another similar study by Banno et al[35] with 68 TEVAR patients, stent grafts with and without proximal bare stents were used in 24 and 44 patients, respectively. Bird-beak configurations were found in 1 patient with proximal bare stents and 29 patients without proximal bare stents. These findings are consistent with our study results where only four bird-beak cases were detected all of which had stent grafts without proximal bare stents.

In addition to stent graft design, several factors including angulation and curvature of the aortic arch, aortic diameter, and landing zone were shown in previous studies to correlate with bird-beak occurrence.[3-7,9,20,30,36,37] In the current study, while device selection likely influenced bird-beak formation in the mentioned cases, other notable characteristics were observed in these patients (Table II), which were shown in our previous study[9] to be risk factors for bird-beak. For patient 7, stent graft oversizing of 5% was used, which is the smallest oversizing value among the simulated patient cohort. For patient 10, proximal landing zone 2 in combination with a relatively small oversizing value of 11% may be the reason for bird-beak. Finally, patient 11 possesses the smallest value of the aortic arch angle, equal to 55.82°, among the simulated patient cases. Patient 11 is one of the youngest patients in the cohort, and the acute aortic arch angle is likely related to the patient's younger age. The highlighted factors are aligned with the findings of our previous study[9] where an inverse correlation was found between the aortic arch angle and bird-beak formation. In addition, it was shown that in most instances larger oversizing can minimize the formation of bird-beak, and landing zones closer to the arch apex (as opposed to straighter sections within the aorta) are more prone to bird-beak.[9] It is worth noting that the classification of these contributing parameters (including stent graft design and aorta geometric parameters) solely based on their values for risk stratification is not possible due to the presence of complex interactions[9] between the parameters. Therefore, computational simulations of TEVAR play a crucial role in predicting bird-beak in these patients.

In this study to further investigate the effect of stent graft selection, additional simulations were run for the three patient cases with bird-beak configuration by replacing the Zenith TX2 with Zenith Alpha devices of same diameters. Although in one of the cases replacing the Zenith TX2 with the Zenith Alpha device did not result in a noticeable change in bird-beak length and angle, in the second case, it significantly reduced the bird-beak length and angle, and in the third case, it completely resolved the presence of bird-beak.

Comparison of simulation results with the surgical outcomes in Figs 3 and 4 showed good agreement between the simulated and postoperative CT images. It was demonstrated that the implemented computational framework can predict the proximal position of the deployed stent graft, including protrusion of the proximal bare stents and presence of bird-beak, accurately. For cases with formed bird-beak configurations, the length and angle of the bird-beak were measured in the simulated results and compared with the postoperative measurements, as shown in Table III. The prediction error ranges between 5.7% and 9.7% for the bird-beak length and between 14.6% and 23.5% for the bird-beak angle.

This study provides evidence that our computational framework can predict the presence or absence of bird-beak configuration in TEVAR using the preoperative CT images. In addition, the computational framework can predict the length of the bird-beak with sufficient accuracy (less than 10% error), whereas the prediction error for the bird-beak angle is within 24%. Considering the accuracy of computational models, various TEVAR scenarios for a patient can be simulated using different stent graft configurations and landing locations. This may be helpful in identifying the optimal scenario

according to the simulated results and can lead to alterations in the decision-making process.

Finite element analysis is a noninvasive method for simulating TEVAR scenarios and potential prediction of surgical outcomes. The computational approach used in this study is clinically significant as it has the potential to enhance surgical planning capabilities with the goal of minimizing bird-beak occurrence. For instance, when the preoperative TEVAR simulation of a patient predicts bird-beak configuration formation, as part of the surgical planning process, additional emphasis can be placed on optimal stent graft oversizing and device selection to reduce the risk of bird-beak. Currently, the initial simulation setup and computational time for a patient is less than 22 hours. Once the initial simulation for a patient is developed, a subsequent simulation with a different stent graft configuration or adjustment of the landing zone can be set up and run relatively quickly (in less than 2 hours and 15 minutes). Therefore, device and landing zone variations can be easily implemented and tested. The median time interval between decision to operate and surgery was previously reported to be 57 days.[38] Therefore, our proposed computational framework can be used within the TEVAR workflow timelines. Although the focus of this study is the repair of thoracic aortic aneurysms, with further investigation a similar approach can potentially be extended to other TEVAR applications such as blunt thoracic aortic injury and aortic dissection.

Study limitations. A number of inherent limitations exist in the implemented computational framework. A uniform wall thickness was used throughout the aorta. The effect of tissues and structures surrounding the thoracic aorta was approximated through applying numerical damping in the simulations. In addition, homogeneous material properties were used in the aorta. Simplifications were made in the computational models to neglect the hemodynamic effects and only apply a static mean arterial pressure of 93 mm Hg. Because patient-specific data on lowering blood pressure during stent graft deployment were not available, only the mean arterial pressure was considered in all simulations. However, due to the equilibrium of static pressure loads on the luminal surface and protruded undersurface of the graft at the bird-beak site, it is expected that considering patient-specific blood pressure values would not have an impact on bird-beak results. Previous studies have shown the impact of hemodynamics on the bird-beak configuration gap over time.[39,40] However, the focus of this study was the formation of bird-beak upon stent graft deployment, and the evolution of bird-beak over time into more serious complications (ie, device migration and collapse, and type Ia endoleak) would require further analysis through implementation of fluid structure interactions.

Considering the limited number of bird-beak cases in our patient cohort, an extended retrospective study that would include more patients with a variety of aortic geometries and stent graft types may result in additional bird-beak cases for further analysis and better estimation of our prediction accuracy. Given the potential of this computational method for clinical translation, including devices from other manufacturers may provide insight into the relationship between design parameters and stent graft apposition and will be instructive for optimal stent graft selection for each patient. Furthermore, this study can benefit from patient-specific benchtop models to deploy and assess the behavior of the stent graft within the aorta. This will be considered as part of future directions of this study.

CONCLUSIONS

Patient-specific TEVAR finite element computational simulations of 12 patients showed good agreement between computationally simulated results and postoperative CT images. Bird-beak configuration was present in 3 of 12 simulated patients. It is speculated that the formation of bird-beak in these patients was related to using Zenith TX2 devices that lack proximal bare stents. Additional risk factors in these patients, including small stent graft oversizing, small aortic arch angle values, and landing zones close to the arch apex, may have played a role. The simulation results confirm that our computational models can predict accurately the final proximal position of the deployed stent graft during TEVAR. The accuracy of our computational simulations in predicting the size of a formed bird-beak was tested, resulting in over 90% and 76% accuracy in the prediction of the bird-beak length and angle, respectively. The implemented TEVAR computational simulations can provide insight into the preoperative planning process with the goal of minimizing bird-beak occurrence.

AUTHOR CONTRIBUTIONS

Conception and design: NS, DR, TF, CA
Analysis and interpretation: NS, DR, TF, CA
Data collection: NS, TF
Writing the article: NS
Critical revision of the article: NS, DR, TF, CA
Final approval of the article: NS, DR, TF, CA
Statistical analysis: Not applicable
Obtained funding: TF, CA
Overall responsibility: NS

REFERENCES

1. Marrocco-Trischitta MM, Spampinato B, Mazzeo G, et al. Impact of the bird-beak configuration on postoperative outcome after thoracic endovascular aortic repair: a meta-analysis. J Endovasc Ther 2019;26:771-8.
2. Boufi M, Alexandru G. Commentary: bird beak after TEVAR: hostile or benign sign? J Endovasc Ther 2019;26:779-81.

3. Nauta FJH, Conti M, Kamman AV, et al. Biomechanical changes after thoracic endovascular aortic repair in type B dissection: a systematic review. J Endovasc Ther 2015;22:918-33.
4. Pasta S, Scardulla F, Rinaudo A, et al. An in vitro phantom study on the role of the bird-beak configuration in endograft infolding in the aortic arch. J Endovasc Ther 2016;23:172-81.
5. Ueda T, Fleischmann D, Dake MD, Rubin GD, Sze DY. Incomplete endograft apposition to the aortic arch: bird-beak configuration increases risk of endoleak formation after thoracic endovascular aortic repair. Radiology 2010;255:645-52.
6. Sze DY, van den Bosch MAAJ, Dake MD, et al. Factors portending endoleak formation after thoracic aortic stent-graft repair of complicated aortic dissection. Circ Cardiovasc Interv 2009;2:105-12.
7. Hsu HL, Chen CK, Chen PL, et al. The impact of bird-beak configuration on aortic remodeling of distal arch pathology after thoracic endovascular aortic repair with the Zenith Pro-Form TX2 thoracic endograft. J Vasc Surg 2014;59:80-8.
8. Lee WA, Martin TD, Hess PJ, Beaver TM, Klodell CT. First United States experience of the TX2 Pro-Form thoracic delivery system. J Vasc Surg 2010;52:1459-63.
9. Shahbazian N, Romero DA, Forbes TL, Amon CH. Identification of geometric and mechanical factors predictive of bird-beak configuration in thoracic endovascular aortic repair using computational models of stent-graft deployment. JVS Vasc Sci 2022;3:259-73.
10. Menichini C, Pirola S, Guo B, Fu W, Dong Z, Xu XY. High wall stress may predict the formation of stent-graft-induced new entries after thoracic endovascular aortic repair. J Endovasc Ther 2018;25:571-7.
11. Auricchio F, Conti M, Marconi S, Reali A, Tolenaar JL, Trimarchi S. Patient-specific aortic endografting simulation: from diagnosis to prediction. Comput Biol Med 2013;43:386-94.
12. Qiao Y, Fan J, Ding Y, Luo PK, Zhu T, Luo K. A primary computational fluid dynamics study of pre- and post-TEVAR with intentional left subclavian artery coverage in a type B aortic dissection. J Biomech Eng 2019;141:111002.
13. Sanford RM, Crawford SA, Doyle MG, Amon CH, Forbes TL. Computational simulations to predict fenestrated stent graft rotation on deployment. J Vasc Surg 2017;66:e82.
14. Sanford RM, Crawford SA, Genis H, Doyle MG, Forbes TL, Amon CH. Predicting rotation in fenestrated endovascular aneurysm repair using finite element analysis. J Biomech Eng 2018;140:091004.
15. Romarowski RM, Conti M, Morganti S, et al. Computational simulation of TEVAR in the ascending aorta for optimal endograft selection: a patient-specific case study. Comput Biol Med 2018;103:140-7.
16. Perrin D, Badel P, Orgeas L, et al. Patient-specific simulation of endovascular repair surgery with tortuous aneurysms requiring flexible stent-grafts. J Mech Behav Biomed Mater 2016;63:86-99.
17. Zhao S, Gu L, Froemming SR. Performance of self-expanding Nitinol stent in a curved artery: impact of stent length and deployment orientation. J Biomech Eng 2012;134:071007.
18. Shahbazian N, Doyle MG, Forbes TL, Amon CH. A modeling framework for computational simulations of thoracic endovascular aortic repair. Int J Numer Method Biomed Eng 2023;39:e3578.
19. Upchurch GR, Escobar GA, Azizzadeh A, et al. Society for Vascular Surgery clinical practice guidelines of thoracic endovascular aortic repair for descending thoracic aortic aneurysms. J Vasc Surg 2021;73:55S-83S.
20. Shahbazian N. The Role of Geometric and Mechanical Properties in Bird-Beak Configuration Formation in Thoracic Endovascular Aneurysm Repair. Thesis. University of Toronto; 2022.
21. Pinter C, Lasso A, Fichtinger G. Polymorph segmentation representation for medical image computing. Computer Methods Programs Biomed 2019;171:19-26.
22. Schroeder WJ, Maynard R, Geveci B. Flying edges: a high-performance scalable isocontouring algorithm, 2015 IEEE 5th Symposium on Large Data Analysis and Visualization (LDAV). Chicago, IL 2015. p. 33-40.
23. Taubin G, Zhang T, Golub G. Optimal surface smoothing as filter design. In: Buxton B, Cipolla R, editors. Computer Vision—ECCV '96. Vol. 1064. Lecture Notes in Computer Science. Springer Berlin Heidelberg; 1996. p. 283-92.
24. Cook Medical. Zenith physician's pocket reference guide. Bloomington, IN: Cook Medical; 2017.
25. Raghavan ML, Ma B, Fillinger MF. Non-invasive determination of zero-pressure geometry of arterial aneurysms. Ann Biomed Eng 2006;34:1414-9.
26. Feher J. Vascular function. In: Quantitative Human Physiology. Elsevier; 2012. p. 498-507.
27. Livermore Software Technology, Livermore Software Technology Corporation, LS-Dyna Keyword User's Manual. Livermore Software Technology Corporation (LSTC); 2018. Available at: https://ftp.lstc.com/anonymous/outgoing/jday/manuals/LS-DYNA_manual_Vol_I_R7.0.pdf. Accessed June 23, 2023.
28. Chen T, Lancaster M, Lin DSY, Doyle MG, Forbes TL, Amon CH. Measurement of frictional properties of aortic stent grafts and their delivery systems. J Med Devices 2019;13:021008.
29. Vad S, Eskinazi A, Corbett T, McGloughlin T, Vande Geest JP. Determination of coefficient of friction for self-expanding stent-grafts. J Biomech Eng 2010;132:121007.
30. Boufi M, Guivier-Curien C, Deplano V, et al. Risk factor analysis of bird beak occurrence after thoracic endovascular aortic repair. Eur J Vasc Endovasc Surg 2015;50:37-43.
31. Kudo T, Kuratani T, Shimamura K, Sawa Y. Determining the optimal proximal landing zone for TEVAR in the aortic arch: comparing the occurrence of the bird-beak phenomenon in zone 0 vs zones 1 and 2. J Endovasc Ther 2020;27:368-76.
32. Kotelis D, Brenke C, Wörz S, et al. Aortic morphometry at endograft position as assessed by 3D image analysis affects risk of type I endoleak formation after TEVAR. Langenbecks Arch Surg 2015;400:523-9.
33. Lin LIK. A concordance correlation coefficient to evaluate reproducibility. Biometrics 1989;45:255.
34. Kudo T, Kuratani T, Shimamura K, et al. Type 1a endoleak following zone 1 and zone 2 thoracic endovascular aortic repair: effect of bird-beak configuration. Eur J Cardiothorac Surg 2017;52:718-24.
35. Banno H, Akita N, Fujii T, et al. Proximal bare stent may reduce bird-beak configuration, which is associated with distal migration of stent graft in the aortic arch. Ann Vasc Surg 2019;56:108-13.
36. Pasta S, Raffa GM, D'Ancona G, Pilato M. Commentary: the bird-beak stent-graft configuration: the end of aortic arch endograft collapse? J Endovascular Ther 2014;21:803-4.
37. Frohlich MM, Suh GY, Bondesson J, et al. Thoracic aortic geometry correlates with endograft bird-beaking severity. J Vasc Surg 2020;72:1196-205.
38. Sadat U, Hayes P, Gaunt M, Varty K, Boyle J. Assessment of preoperative delays in the management of elective abdominal aortic aneurysms. Annals 2008;90:65-8.
39. Pasta S, Cho JS, Dur O, Pekkan K, Vorp DA. Computer modeling for the prediction of thoracic aortic stent graft collapse. J Vasc Surg 2013;57:1353-61.
40. van Bogerijen GHW, Auricchio F, Conti M, et al. Aortic hemodynamics after thoracic endovascular aortic repair, with particular attention to the bird-beak configuration. J Endovas Ther 2014;21:791-802.

Submitted Dec 16, 2022; accepted Apr 3, 2023.